Thermochimica Acta 719 (2023) 179414

Contents lists available at ScienceDirect

Thermochimica Acta

journal homepage: www.elsevier.com/locate/tca

Fast scanning calorimetry on volatile carbon-based materials

Valerio Di Lisio [a], Balthasar Braunewell [b], Cristina Macia-Castello [b], Margherita Simoni [c], Roberto Senesi [c], Felix Fernandez-Alonso [a,b,d,*], Daniele Cangialosi [a,b,*]

[a] Donostia International Physics Center (DIPC), Paseo Manuel de Lardizabal 4, Donostia - San Sebastian 20018, Spain
[b] Centro de Fisica de Materiales (CSIC-UPV/EHU), Paseo Manuel de Lardizabal 5, Donostia - San Sebastian 20018, Spain
[c] Department of Physics and NAST Centre, Università degli Studi di Roma Tor Vergata, Via della Ricerca Scientifica 1, Rome 00133, Italy
[d] IKERBASQUE, Basque Foundation for Science, Plaza Euskadi 5, Bilbao 48009, Spain

ARTICLE INFO

Keywords:
Fast scanning calorimetry (FSC)
Differential scanning calorimetry (DSC)
Volatile carbon-based materials
Sample encapsulation & preparation
Crystallization
Glass transition

ABSTRACT

This work introduces a new sample-preparation methodology to investigate volatile materials with fast scanning calorimetry (FSC). The protocol consists of a two-step process involving the embedding of the specimen in an inert silicone-oil-based matrix followed by gold sputtering, in order to ensure full encapsulation and isolation from the surrounding environment. This novel approach is tested thoroughly on a series of three carbon-based materials – resorcinol, corannulene and perylene. In addition to establishing the validity of our methodology, the FSC data also gives access to new and hitherto unexplored regimes of thermodynamic stability and metastability in these materials, including the emergence of glassy states, cold crystallization, and solid-to-solid transformations.

1. Introduction

The thermodynamic state of liquids cooled down below their melting temperature (hereafter T_M) spontaneously evolves towards the lowest free-energy minimum, that is, the most stable crystal [1]. The kinetic pathway entailed in the transformation from liquid to crystal may encompass a very wide range of timescales: from picoseconds, as it is the case of archetypal systems such as water [2,3], metals [4–6] or polyethylene, one of the simplest known polymers [7]; to unfeasibly long ones, as it is found in atactic polymers [8]. Within this broad range of timescales of crystallization, the vast majority of liquids fall into the class of systems where crystallization can be avoided at a given threshold cooling rate, thereby opening the door to the emergence of a metastable supercooled liquid transforming into a non-equilibrium glass at lower temperatures – a phenomenon known as glass transition or vitrification [1,9,10]. Thermophysical techniques such as Differential Scanning Calorimetry (DSC) [11] have been typically limited to maximum cooling rates up to a few K s^{-1}. These experimental conditions are often insufficient to preserve the metastable liquid state below T_M, thereby preventing a robust isolation of the supercooled liquid and the glass. The more recent development of Fast Scanning Calorimetry (FSC) [12] using ultra-small specimens to attain heating/cooling rates as high as thousands of K s^{-1} has changed the above situation in a substantive manner, thereby enabling the exploration of hitherto-unknown kinetic pathways that circumvent incipient crystallization upon cooling below T_M.

In the present work, we extend the realm of applicability of FSC to study the thermophysical behavior of a series of three highly volatile carbon-based materials: Resorcinol, a monocyclic aromatic diol decorated with hydrogen-bonding motifs; as well as Corannulene and Perylene, two (nearly isobaric) polycyclic aromatic hydrocarbons with a distinctly different molecular topology. Beyond the methodological developments described herein, we also seek to explore for the first time their ability and propensity to resisting crystallization. In so doing, we also assess the potential of FSC for the further study of this class of materials, which has received little attention to date owing to their relatively high vapor pressures in their condensed phases and associated propensity to 'boil-off' during calorimetric studies. To circumvent the above experimental difficulties, we tackle the aforementioned issue of sample evaporation by developing a new methodology based on encapsulation and isolation from the immediate surroundings.

2. Experimental & methods

Resorcinol (≥99% purity), Perylene (≥99% purity) and Polydimethylsiloxane (PDMS, viscosity 10^5 cP) were provided by Sigma

* Corresponding authors at: Centro de Fisica de Materiales (CSIC-UPV/EHU), Paseo Manuel de Lardizabal 5, Donostia - San Sebastian 20018, Spain.
E-mail addresses: felix.fernandez@ehu.eus (F. Fernandez-Alonso), daniele.cangialosi@ehu.eus (D. Cangialosi).

https://doi.org/10.1016/j.tca.2022.179414
Received 21 October 2022; Received in revised form 5 December 2022; Accepted 5 December 2022
Available online 9 December 2022

Aldrich and used as received. Corannulene was produced using the synthetic procedures described in previous works and references therein [13–15], and further purified by vacuum sublimation at 448 K and 10^{-3} mbar. The molecular structures of these three carbon-based compounds are shown in Fig. 1.

DSC was performed by means of a Q2000 system from TA Instruments, equipped with an intra-cooler to operate over the temperature range 193–873 K under a dry-nitrogen atmosphere using a gas-flow rate of 50 ml/min. DSC samples of Resorcinol, Corannulene and Perylene were prepared by hermetically sealing about 10 mg of the respective powder specimen in Aluminium pans. Thermograms were recorded at heating and cooling rates of 3 K min^{-1}.

FSC was performed with a Mettler–Toledo Flash DSC 1 equipped with an intra-cooler to operate between 173 K and 723 K. The FSC system comprised a Leica M60 optical microscope operating at a magnification of 400X. A Leica IC80 HD video camera was used to acquire chip micrographs. The sample chamber was purged with dry nitrogen at a flow rate of 20 ml/min. FSC specimens were prepared following two different procedures. The first involved direct deposition of a sample mass of about 100 ng directly onto a Mettler–Toledo UFS1 chip. The resulting samples are henceforth named *Resor*, *Cora* and *Peryl* for Resorcinol, Corannulene and Perylene, respectively. The alternative procedure involved the deposition of a small drop of PDMS (about 200 μm diameter) onto the sample area of the chip. Subsequently, samples of about 100 ng were deposited and dispersed within the PDMS drop. Adding silicon oil, apart from favoring heat transfer [16], can be used to avoid sample evaporation, a procedure already adopted with success in the study of amino-acid melting [17]. After PDMS deposition, the ceramic part of the FSC chip was masked with tape, in order to restrict the subsequent deposition of gold only to sample and reference membranes. Gold sputtering was performed by means of an Edwards Scancoat Six, operating at a voltage of 1.5 kV and a current of 20 mA for a total deposition time of ten minutes. To avoid the overheating of the chip during the process, gold sputtering was divided into two steps of five minutes, separated by a five-minute interval. In line with the naming convention introduced above, gold-coated specimens are hereafter referred to as *Res_Au*, *Cora_Au*, and *Peryl_Au*. This procedure is further illustrated graphically in Fig. 2. The resulting configuration aims at providing a hermetic seal of the sample on the FSC chip to prevent unwanted evaporation upon heating, as presented in more detail in the Results Section below.

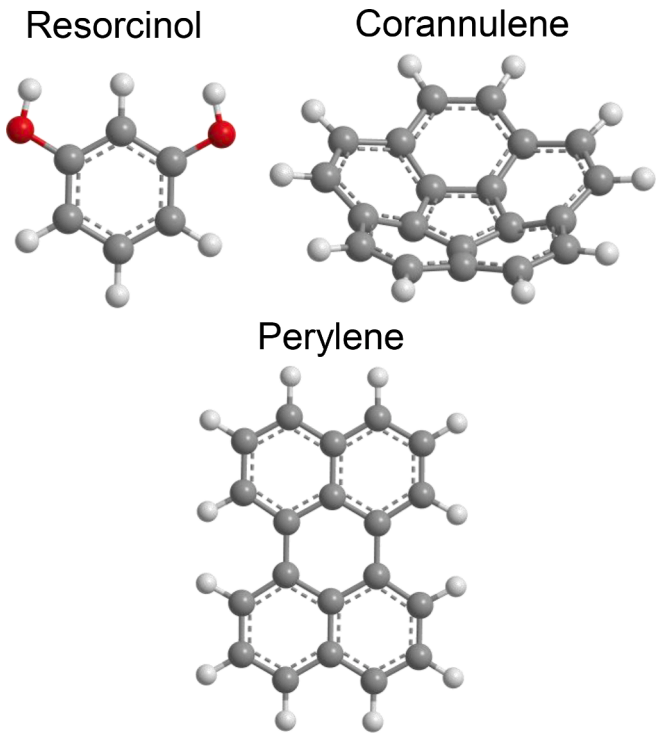

Fig. 1. Molecular structures of the three carbon-based molecular materials of relevance to this work. Black, white, and red are used to denote carbon, hydrogen and oxygen atoms, respectively.

Res, *Cora* and *Peryl* were scanned at heating and cooling rates of 1000 K s^{-1} over the temperature range 183–403 K, 183–553 K and 183–563 K, respectively. The scans were repeated three-to-five times depending on the sample. Regarding the gold-sputtered samples, *Res_Au* was scanned at 1000 K s^{-1} in the range 183–403 K, *Cora_Au* was heated at 1000 K s^{-1} and cooled at 4000 K s^{-1} in the range 183–563 K, and *Peryl_Au* heated at 1000 K s^{-1} and cooled at 10000 K s^{-1} in the range 183–573 K. All gold-sputtered samples were cycled five times to confirm the absence of mass loss. The protocol introduced by Schawe [18] was used to assess thermal lag in those systems exhibiting vitrification. This procedure is based on the determination of a limiting fictive temperature T_f, that is, the temperature at which a glass cooled down at a certain rate would be at equilibrium [19]. For a glass heated immediately after cooling, T_f on cooling and heating must coincide. Hence, any differences in T_f obtained on heating and cooling must correspond to twice the thermal lag. For resorcinol and corannulene specimens of mass ~100 ng, this procedure gave thermal lags of ±2.5 K, a result which was independent of sample configuration. Although perylene could not be vitrified, this thermal lag applies as well, given the similar mass used for this sample.

To provide a stringent test of the equivalence of the two sample-preparation procedures, the spontaneous fluctuations of the main α relaxation associated to the glass transition of *Res* and *Res_Au* were characterized in terms of the frequency-dependent complex thermal susceptibility, that is, the complex specific heat. A step-response protocol [20–22] was used for both specimens, consisting of a down-step of 2 K at 200 K s^{-1} followed by an isothermal for 1.6284 s, corresponding to a base frequency of ~0.61 Hz. The temperature range was 273-223 K. The real (C_p') and imaginary (C_p'') parts of C_p^*, the complex specific heat, were assessed for the base frequency and higher-order harmonics by means of a Fourier-transform relationship of the form:

$$C_p^*(\omega) = C_p'(\omega) - iC_p''(\omega) = \frac{\int_0^{t_p} HF(t)\, e^{-i\omega t}\, dt}{\int_0^{t_p} \beta(t)\, e^{-i\omega t}\, dt} \quad (1)$$

where t_p is the period of the step, $HF(t)$ and $\beta(t)$ are the heat flow rate and the instantaneous cooling rate, respectively, and ω is the angular frequency. The Fourier-transform relation of Eq. (1) also allows a

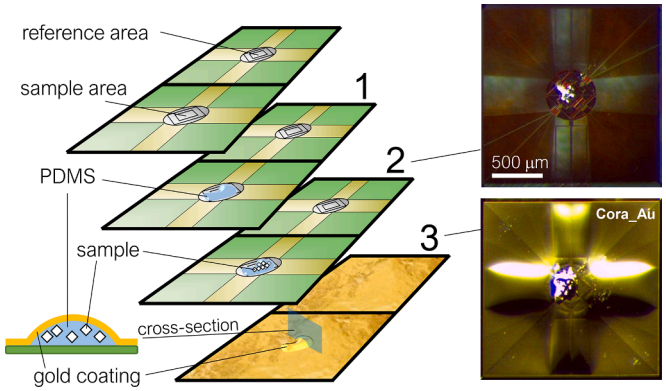

Fig. 2. Cartoon illustrating the sequence of steps to achieve sample encapsulation: bare FSC chip (top); PDMS deposition (1); addition of sample to the PDMS drop (2); and final gold-coated specimen (3), also drawn schematically at the bottom-left of the figure. The two photographs on the right illustrate the physical appearance of actual samples under the microscope. For further details see the main text.

determination of the reversing specific heat C_p^{rev} from the modulus of the complex number C_p^*. In practice, these experimental data in the time domain enable the use of Eq. (1) by taking recourse to discrete Fast-Fourier-Transform (FFT) numerical algorithms. The frequency dependence of the glass-transition temperature in the linear-response regime is quantified via the definition of a "dynamic glass transition temperature" (T_g^{dyn}). This quantity was determined as the half-step in $C_p^{rev}(\omega)$. Here, it is worth mentioning that the underlying cooling rate applied in the step-response protocol amounts to ~1.2 K s^{-1}. At this relatively modest rates, thermal lags have been shown to be practically negligible [18].

3. Results

In order to assess the efficiency of our new sealing procedure through PDMS deposition and subsequent gold sputtering, a series of three, intermediate molecular-weight carbon-based materials with different crystallization and evaporation kinetics were utilized. As shown in Fig. 3, Resorcinol is a diphenol characterized by a melting temperature of T_M = 383 K [23], slow crystallization kinetics and a high boiling temperature of 550 K. This behavior is linked to the bidentate nature of its hydroxyl groups and their ability to form moderately strong intermolecular hydrogen bonds [24]. Corannulene and Perylene are nearly isobaric polycyclic aromatic hydrocarbons with a comparable melting temperature of T_M ~ 550 K [25]. As shown in Fig. 1, the presence of a pentagonal unit at the center of the Corannulene molecule ($C_{20}H_{10}$) gives rise to a characteristic bowl-shaped topology, as opposed to the flat structure seen in Perylene ($C_{20}H_{12}$) and the vast majority of other known polycyclic aromatic hydrocarbons [13,14]. These differences offer a convenient means of assessing in a controlled manner the effects of molecular topology and curvature on thermophysical behavior for this class of materials, characterized by relatively weak and rather unspecific intermolecular van-der-Waals interactions.

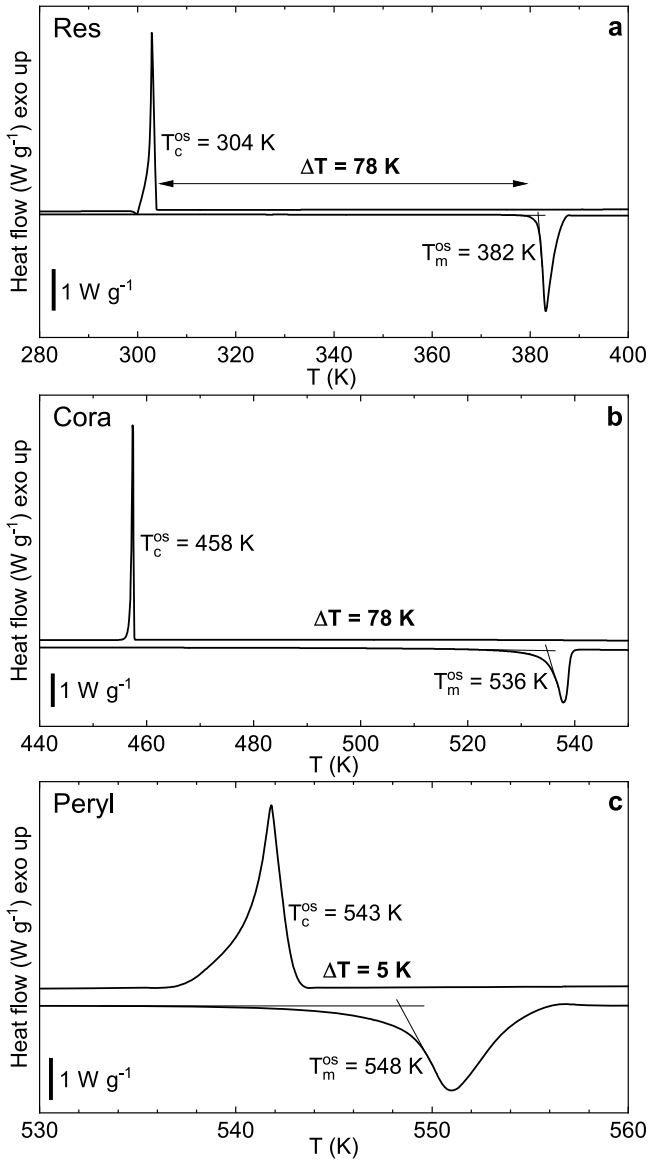

Fig. 3. DSC curves of hermetically sealed samples, measured at heating and cooling rates of 3 K min^{-1}.

In all cases covered in this work, their tendency to crystallize was assessed by means of standard DSC in terms of the hysteresis between the temperatures of melting (T_M) and crystallization (T_C), as shown in Fig. 3. On cooling at 3 K min^{-1}, Resorcinol exhibits a large hysteresis and can be supercooled by 78 K, with T_C/T_M ~ 0.8 indicating slow nucleation kinetics. In contrast, Corannulene and (above all) Perylene show a reduced hysteresis resulting in a supercooling gap of 78 K and 5 K and T_C/T_M ~ 0.86 and 0.99, respectively. Altogether, the characterization via standard DSC indicates that in all three cases, cooling rates of the order of 3 K min^{-1} invariably lead to crystallization before vitrification can be observed.

The above thermo-physical scenario can be modified quite substantially by accessing a fast-cooling regime beyond the conditions afforded by conventional DSC. Fig. 4 shows multiple FSC heating/cooling cycles at a fixed rate of 1000 K s^{-1}, except for the cooling ramps of *Cora_Au* and *Peryl_Au* (4000 and 10,000 K s^{-1}, respectively). The thermograms obtained for the as-deposited samples *Res*, *Cora* and *Peryl* are presented in the left panels a, c and e. Direct visual inspection of the data from the samples directly deposited on the chip without any encapsulation indicates that these suffer from severe material loss, as evidenced by the gradual suppression of the heat-flow-rate signal between consecutive heating cycles. This behavior is most pronounced for *Peryl*, exhibiting practically complete signal loss already after the first heating ramp. The optical micrographs for *Res* shown in the inset of Fig. 4(a) unequivocally show that the main cause of signal loss is related to sample evaporation in the melt, followed by deposition on the cold part of the chip. This effect is further confirmed by the appearance of a distinct condensation halo around the active area, most apparent in *Res* after the fifth heating cycle.

To overcome sample evaporation during the FSC experiments, we tested in detail our specific procedure based on embedding the specimens in PDMS followed by gold sputtering, as introduced above in Section 2. Figs. 2 and 4(b) show a set of optical micrographs of gold-sputtered chips of *Cora_Au* and *Res_Au*, respectively. The sealing procedure succeeded whenever the chip was covered by a continuous gold film, with a dome covering the sample dispersed in PDMS located on the active area. In this way, the sample is entrapped in a closed chamber formed between the chip and the gold dome. It is important to note that for a successful procedure, the edges of the dome must stay within the active area. Otherwise, uniform heating cannot be achieved and portions of the specimen can migrate to cooler parts outside the active area, resulting in a loss of sample mass. Furthermore, it is worth emphasizing the importance of employing both PDMS embedding and gold sputtering to guarantee sample integrity. If only PDMS embedding is carried out, the sample can migrate to the free surface and evaporate due to the fluidity of PDMS. Here, we underline the difference with previous works showing that simple PDMS embedding was sufficient to prevent the evaporation of amino acids above melting [17]. In contrast, likely owing to the high vapor pressure above melting of the systems investigated in our study, sample preparation exclusively based on PDMS embedding resulted in gradual sample loss after consecutive heating/cooling cycles.

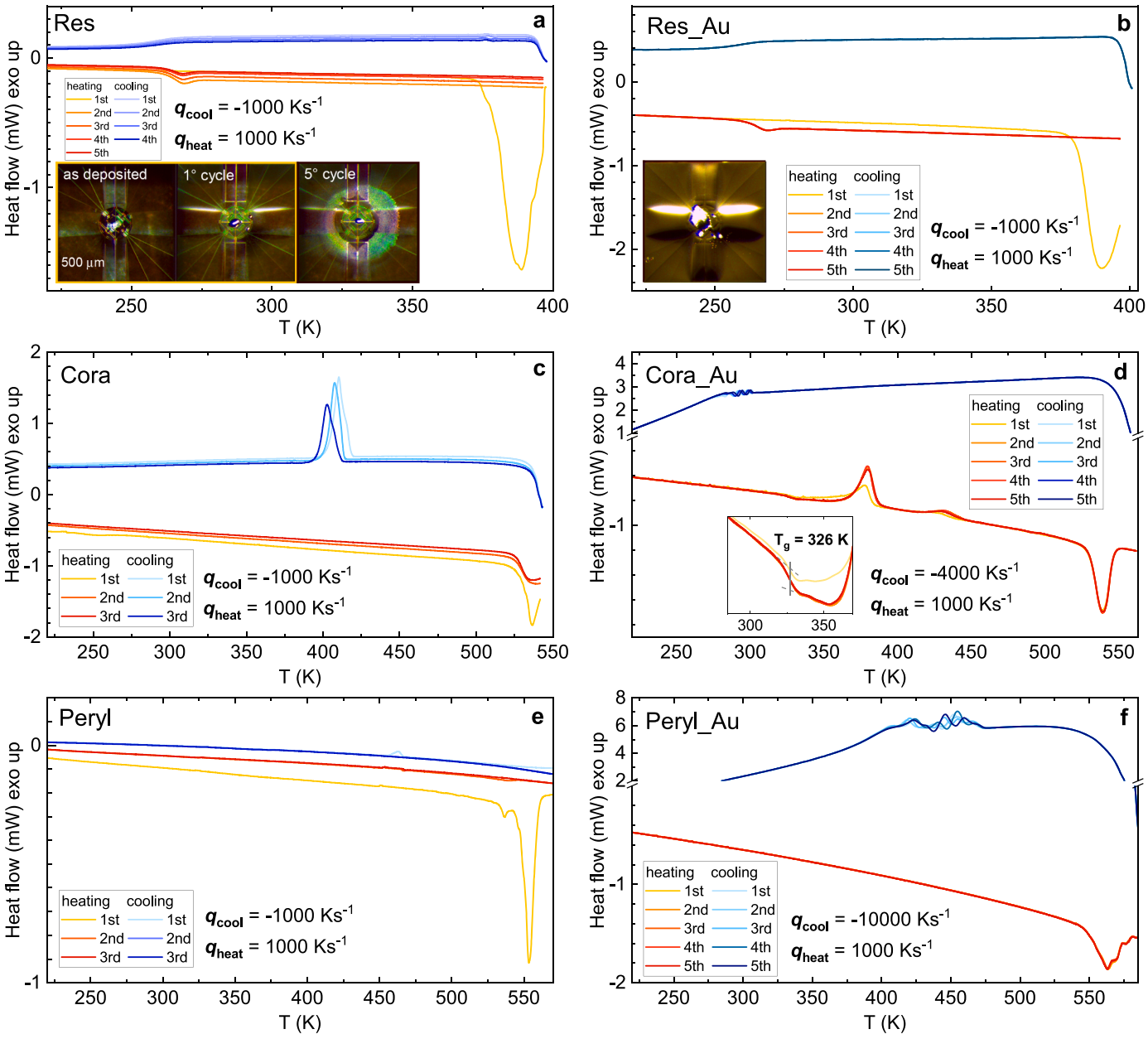

Fig. 4. FSC curves of consecutive heating/cooling cycles for as-deposited (left panels) and encapsulated samples (right panels). The optical micrographs of Resorcinol were taken on the as-deposited sample after the first and the fifth heating cycles. The heating rate is in all cases 1000 K/s. The cooling rate is 1000 K/s for the as-deposited samples and 4000 K/s for the PDMS embedded/gold sputtered samples.

Likewise, direct sputtering of gold on the sample does not lead to satisfactory results. In this case, the rough and ill-defined interfaces characteristic of friable polycrystalline powders are hardly conducive to uniform gold deposition. Differences in thermal-expansion coefficients between sample and gold can, in this situation, result in the formation of cracks on the gold film, ultimately leading to sample leakage and unwanted evaporation. This event is prevented by using fluid PDMS, owing to its ability to reduce the mechanical stress that would otherwise exist in a rigid sample in direct contact with the surrounding gold layer.

As further illustration of the above, panels b, d and f in Fig. 4 present FSC scans for the gold-sputtered samples. Relative to the as-deposited samples, clear and substantial differences emerge: all PDMS embedded/gold-sputtered samples show stable and reproducible heat-flow-rate signals in consecutive cycles, indicating the effectiveness of the sealing procedure. However, it is important to note that PDMS embedding does not result in any changes to thermo-physical properties, as the melting temperatures of as-deposited and PDMS-embedded samples coincide (see Fig. 4). This result implies that no mixing at the molecular level between the investigated samples and PDMS takes place. Sample stability in this configuration also allows us to conclude that *Res_Au* can been kept amorphous over long time scales, thereby enabling (for the first time) the study of hitherto-unexplored vitrification phenomena. Specifically, *Res_Au* shows the typical signature of the glass transition, namely, a step in the heat-flow rate on both heating and cooling. The resulting glass transition temperature, T_g, taken at the mid-step of the specific heat jump, is 259 K and 264 K on cooling and heating, respectively. Furthermore, repeated heating/cooling cycles show identical C_p scans, where no sign of crystallization/melting can be detected. These results highlight the strong resistance to crystallization of resorcinol.

Contrary to the above phenomenology, the FSC data on *Peryl_Au* show the fastest crystallization kinetics among all systems investigated

in this work and, as such, this material could not be obtained in amorphous form. Melt crystallization occurs even at the maximal nominal cooling rates allowed by the technique (− 10,000 K s^{-1}). This behavior is evident from the FSC scans obtained on cooling from the melt, where a crystallization exotherm can be detected over a rather broad temperature range between 400 and 470 K. The FSC heating cycles at 1000 K s^{-1} serve as further confirmation of the above: only melting can be observed above 548 K, and no signatures of the glass transition can be discerned from the experimental data.

The curved polycyclic hydrocarbon *Cora_Au* exhibits an intermediate behavior relative to *Res_Au* and *Peryl_Au*. Specifically, it can be kept amorphous on cooling at 4000 K s^{-1}, thereby allowing access to a glassy state. In the context of previous works on this material [13,14] and its topological relation to *Peryl_Au*, this is a rather unprecedented result which could only be obtained by using the fast cooling rates afforded by FSC in combination with the sealed-sample configuration presented in this work. The fully amorphous nature of rapidly cooled *Cora_Au* is further evidenced by the absence of crystallization on cooling. Multiple heating/cooling scans deliver identical features, once more confirming the reliability of our encapsulation protocol. Successive FSC heating scans of *Cora_Au* evince the presence of a very rich phenomenology. Starting from low temperatures, we first observe a step in the heat-flow rate at 326 K, corresponding to the glass transition of fully amorphous corannulene. At 382 K and 430 K, two exothermic peaks are found, which can be assigned to cold crystallization and secondary crystallization/solid-solid transformation, respectively. The so-formed crystal phase begins to melt at 530.5 K, in line with DSC (T_m^{DSC} = 535.9 K) and the as-deposited FSC sample (T_m^{FSC} = 529.1 K). The melting and glass transition temperatures obtained in the FSC and DSC experiments on all samples of relevance to this work are shown in Table 1. These figures further confirm the adequacy of our encapsulation procedure, as well as provide new and fresh data on both Resorcinol and Corannulene.

Altogether, our results serve to establish marked differences in thermo-physical response between a hydrogen-bond-forming aromatic hydrocarbon (with a poor predisposition for crystallization) and the two investigated polycyclic aromatic hydrocarbons Perylene and Corannulene. The planar and highly symmetric structure of Perylene is reflected in its high tendency to crystallize, unavoidable even at cooling rates of thousands of K s^{-1}. In contrast, the bowl-shaped symmetry of an otherwise rigid Corannulene molecule enables this material to be fully amorphized and transformed into a glass by FSC.

As a general feature, we have shown that at a qualitative level the thermophysical properties of all investigated samples are in line with those obtained by standard DSC. However, it is worth pointing out that, so far, we have discussed kinetic transformations, which generally bear a certain amount of hysteresis. This is clearly evident in crystallization, where the degree of supercooling can be varied vastly by changing the cooling rate. Similar considerations apply to typical kinetic phenomena such as the glass transition, where fast cooling induces vitrification at high temperatures. Furthermore, melting too may be subjected to a certain degree of hysteresis giving rise to crystal superheating. In the following, we provide an additional set of experiments whose primary aim is to further verify whether our encapsulation protocol affects thermophysical characterization and analysis in any fundamental way. To this end, we take a closer look at the temperature dependence of spontaneous fluctuations in the deeply supercooled liquid of Resorcinol.

Table 1
Comparison of observed transition temperatures using DSC and FSC.

Compound	T_g^{FSC} (K)	$T_g^{FSC\_Au}$ (K)	T_m^{DSC} (K)	T_m^{FSC} (K)	$T_m^{FSC\_Au}$ (K)
Resorcinol	264	264	382.0	378.5	382.5
Corannulene	–	326	535.9	529.1	530.2
Perylene	–	–	548.5	548.7	547.4

These are related to the time scale of the main α relaxation, generally associated to the glass transition, and can be investigated by applying step-response methods in FSC to access the frequency-dependent thermal susceptibility, that is, the complex heat capacity $C_p^*(\omega) = C_p'(\omega) + iC_p''(\omega)$. Resorcinol was chosen as a test case because of its stability in the amorphous state, enabling the investigation of its glassy behavior over a wide range of experimental conditions. Fig. 5 shows the frequency-dependent reversing heat capacity C_p^{rev}, approximately equal to C_p' [5], for *Res* (top-left panel) and *Res_Au* (top-right panel). From these data, we obtain the frequency-dependent dynamic-glass-transition temperature taken as the mid-step of C_p^{rev}. This quantity also defines the relaxation rate τ^{-1} of the α process, shown as a function of the inverse temperature for both *Res* and *Res_Au* in the lower panel of Fig. 5. As can be observed, *Res* and *Res_Au* exhibit identical behavior, thus confirming that the sealing procedure does not introduce spurious results. Furthermore, τ^{-1} data conform to the celebrated Vogel–Fulcher–Tammann equation [26–28], describing the super-Arrhenius temperature dependence of the α relaxation process according to

$$\tau^{-1} = \tau_0^{-1} \exp \frac{-D^* T_0}{(T - T_0)} \tag{2}$$

where τ_0, T_0 and D^* are the pre-exponential factor, the Vogel temperature and the kinetic fragility index, respectively. A value of $D^* = 4.11$ classifies Resorcinol as a "fragile" glass-former according to the Angell classification [29], that is, a liquid exhibiting a strong temperature dependence of the relaxation timescale τ.

4. Conclusions & outlook

Sample preparation in FSC can be a challenging task if extensive material characterization is the aim, particularly over repeated heating-cooling cycles [16]. To circumvent the above challenge, the work reported herein provides a new strategy to investigate volatile materials, which otherwise would not be amenable to detailed scrutiny using FSC owing to the small sample sizes required by the technique and their associated (and quite substantial) free-area-to-volume ratios. To this end, we have shown that the embedding of FSC samples in a silicon oil like PDMS followed by gold sputtering can avoid these complications altogether, as evidenced by our experimental results on a series of three carbon-based materials exhibiting a high volatility. Beyond the scope of the present work, we anticipate that this procedure will also be of benefit for the study of a plethora of other cases that so far have not been the subject of detailed investigations via FSC.

Apart from enabling FSC investigations on new classes of materials, our study provides a route to attain otherwise inaccessible metastable states on these by fast cooling. Specifically, we have shown that fully amorphous glassy Corannulene can be obtained by fast cooling, where crystallization from the melt cannot be avoided at the rates accessible by standard DSC. While Perylene cannot be vitrified presumably owing to its highly symmetric structure, we show that cooling at high rates can delay crystallization by up to tens of degrees Kelvin. Finally, we have shown how the rather weak tendency of crystallization of Resorcinol can be used to compare at a quantitative level the glass dynamics of as-deposited and encapsulated specimens, thus providing a stringent test of the validity of the new sample-preparation protocol introduced in this work.

Declaration of Competing Interest

The authors declare that they have no known competing financial interests or personal relationships that could have appeared to influence the work reported in this paper.

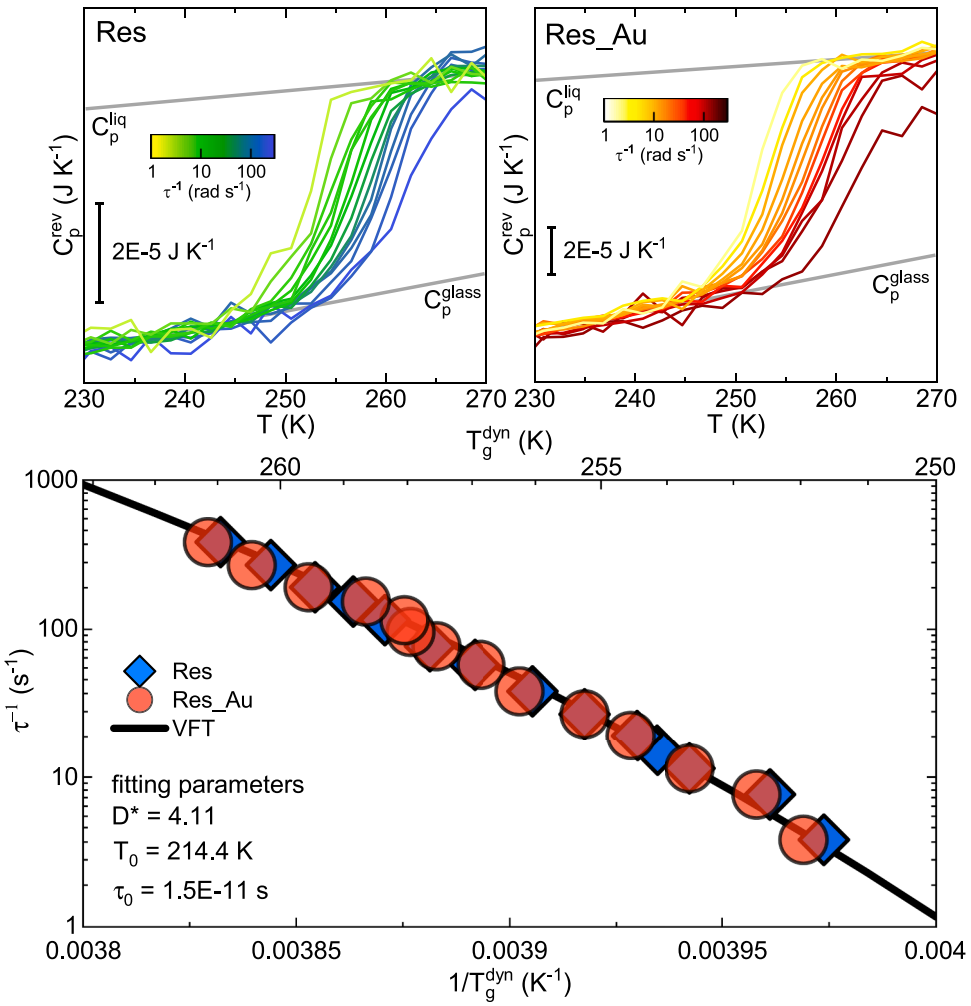

Fig. 5. Quantitative comparison between the frequency-dependent C_p^{rev} of *Res* (top-left panel) and *Res_Au* (top-right panel). The bottom figure shows the temperature dependence of the relaxation rate for both samples. For further details, see the accompanying discussion in the main text.

Data availability

Data will be made available on request.

Acknowledgments

Financial support for this work has been secured through Grants PID2020-114506GB-I00 funded by MCIN/AEI/10.13039/501100011033; TED2021-129457B-I00 funded by MCIN/AEI /10.13039/501100011033 and the European Union NextGenerationEU/PRTR; PIBA-2021-0026 and EC-2022-1-0019, funded by the Basque Government. B.B. thanks the Basque Government for a PREDOCBERRI Ph.D. fellowship. We also acknowledge the financial support received from the IKUR Strategy under the collaboration agreement between Ikerbasque Foundation and the Materials Physics Center on behalf of the Department of Education of the Basque Government.

References

[1] J.W.P. Schmelzer, I.S. Gutzow, Glasses and the Glass Transition, Wiley-VCH, Weinheim, 2011.
[2] G. Johari, A. Hallbrucker, E. Mayer, The glass–liquid transition of hyperquenched water, Nature 330 (6148) (1987) 552–553.
[3] V. Velikov, S. Borick, C. Angell, The glass transition of water, based on hyperquenching experiments, Science 294 (5550) (2001) 2335–2338.
[4] J.F. Löffler, Bulk metallic glasses, Intermetallics 11 (6) (2003) 529–540.
[5] X. Monnier, D. Cangialosi, B. Ruta, R. Busch, I. Gallino, Vitrification decoupling from α-relaxation in a metallic glass, Sci. Adv. 6 (17) (2020) eaay1454.
[6] R. Busch, I. Gallino, Kinetics, thermodynamics, and structure of bulk metallic glass forming liquids, JOM 69 (11) (2017) 2178–2186.
[7] E. Zhuravlev, V. Madhavi, A. Lustiger, R. Androsch, C. Schick, Crystallization of polyethylene at large undercooling, ACS Macro Lett. 5 (3) (2016) 365–370.
[8] U. Gedde, Polymer Physics, Springer Science & Business Media, 1995.
[9] D. Cangialosi, Dynamics and thermodynamics of polymer glasses, J. Phys. Cond. Matt. 26 (15) (2014) 153101.
[10] S. Napolitano, E. Glynos, N.B. Tito, Glass transition of polymers in bulk, confined geometries, and near interfaces, Rep. Prog. Phys. 80 (3) (2017) 036602.
[11] B. Wunderlich, Thermal Analysis of Polymeric Materials, Springer, Berlin, Heidelberg, 2005.
[12] C. Schick, V. Mathot, Fast Scanning Calorimetry, Springer, 2016.
[13] M. Gaboardi, I. Silverwood, B. Braunewell, J. Siegel, F. Fernandez-Alonso, Emergence of dynamical disorder and phase metastability in carbon nanobowls, Carbon 183 (2021) 196–204.
[14] M. Gaboardi, F. Pratt, C. Milanese, J. Taylor, J. Siegel, F. Fernandez-Alonso, The interaction of hydrogen with corannulene, a promising new platform for energy storage, Carbon 155 (2019) 432–437.
[15] A.M. Butterfield, B. Gilomen, J.S. Siegel, Kilogram-scale production of corannulene, Organ. Process Res. Dev. 16 (4) (2012) 664–676.
[16] J.E. Schawe, S. Pogatscher, Material characterization by fast scanning calorimetry: practice and applications. Fast Scanning Calorimetry, Springer, 2016, pp. 3–80.
[17] Y.Z. Chua, H.T. Do, C. Schick, D. Zaitsau, C. Held, New experimental melting properties as access for predicting amino-acid solubility, RSC Adv. 8 (2018) 6365–6372.
[18] J.E. Schawe, Measurement of the thermal glass transition of polystyrene in a cooling rate range of more than six decades, Thermochim. Acta 603 (2015) 128–134.
[19] C.T. Moynihan, P.B. Macedo, C.J. Montrose, P.K. Gupta, M.A. De Bolt, J.F. Dill, B. E. Dom, P.W. Drake, A.J. Eastel, P.B. Elterman, R.P. Moeller, H. Sasabe, J. A. Wilder, Structural relaxation in vitreous materials, Ann. NY Acad. Sci. 279 (1976) 15–35.

[20] M. Merzlyakov, C. Schick, Step response analysis in {DSC}: a fast way to generate heat capacity spectra, Thermochim. Acta 380 (1) (2001) 5–12.
[21] E. Shoifet, G. Schulz, C. Schick, Temperature modulated differential scanning calorimetry - extension to high and low frequencies, Thermochim. Acta 603 (2015) 227–236.
[22] N.G.P.-d. Eulate, V.D. Lisio, D. Cangialosi, Glass transition and molecular dynamics in polystyrene nanospheres by fast scanning calorimetry, ACS Macro Lett. 6 (8) (2017) 859–863.
[23] M.D. Ossowska-Chrusciel, E. Juszysska-Galazka, W. Zajac, A. Rudzki, J. Chrusciel, Mesomorphic properties of resorcinol, J. Mol. Struct. 1082 (2015) 103–113.
[24] R.B. Durairaj, Resorcinol: Chemistry, Technology and Applications, Springer Science & Business Media, 2005.
[25] J.S. Chickos, P. Webb, G. Nichols, T. Kiyobayashi, P.-C. Cheng, L. Scott, The enthalpy of vaporization and sublimation of corannulene, coronene, and perylene at $T = 298.15$ K, J. Chem. Thermodyn. 34 (8) (2002) 1195–1206.
[26] H. Vogel, The temperature dependence law of the viscosity of fluids, Phys. Z 22 (1921) 645–646.
[27] G.S. Fulcher, Analysis of recent measurements of the viscosity of glasses, J. Am. Ceram. Soc. 8 (6) (1925) 339–355.
[28] G. Tammann, W. Hesse, The dependancy of viscosity on temperature in hypothermic liquids, Z. Anorg. Allg. Chem. 156 (4) (1926) 245.
[29] C. Angell, Relaxation in liquids, polymers and plastic crystals strong/fragile patterns and problems, J. Non-Crystalline Solids 131 (1991) 13–31.